Dynamics of liquid CCl_4 from quasi-elastic neutron scattering

1991 J. Phys.: Condens. Matter 3 851

(http://iopscience.iop.org/0953-8984/3/7/009)

J. Phys.: Condens. Matter 3 (1991) 851–863. Printed in the UK

Dynamics of liquid CCl_4 from quasi-elastic neutron scattering

F J Bermejo†, M Alvarez†, M García-Hernández‡, F Mompeán‡, R P White§, W S Howells‡, C J Carlile‡, E Enciso‖ and F Batallan¶

† Consejo Superior de Investigaciones Científicas (CSIC), Instituto de Estructura de la Materia, Serrano 119, E-28006 Madrid, Spain

‡ ISIS Pulsed Neutron Facility, Rutherford Appleton Laboratory, Chilton, Didcot Oxon OX11 0QX, UK

§ Institut Laue–Langevin, 156X, 38042 Grenoble Cédex, France

‖ Departamento Química-Física, Universidad Complutense de Madrid, E-28040 Madrid, Spain

¶ Consejo Superior de Investigaciones Científicas (CSIC), Instituto de Ciencia de Materiales, Serrano 144, E-28006 Madrid, Spain

Received 10 July 1990, in final form 30 November 1990

Abstract. Medium- ($\Delta E = 50$ μeV) and high-resolution ($\Delta E = 15$ μeV) neutron quasi-elastic scattering spectra of liquid CCl_4 at two temperatures within the liquid range are reported. The (mostly coherent) dynamical structure factors are analysed in terms of a model which takes into account the effects of the liquid structure on the single-particle dynamics, and extends the usual rotational diffusion approximations. Such an extension was found to be necessary in order to reconcile the measured dynamical parameters with those available from NMR relaxation.

1. Introduction

Liquid carbon tetrachloride is perhaps the simplest and most widely studied molecular liquid. Because of its T_d point-group symmetry the intermolecular potential may be represented in terms of a sum of additive pair interactions of Lennard-Jones type with a relatively small electrostatic contribution arising from the permanent octupole moment [1]. It can therefore be considered as the closest molecular analogue to liquefied rare gases. Although its structural details can be readily understood by means of computer simulations or approximate integral-equation approaches, the details concerning the molecular dynamics (centre-of-mass motions and molecular reorientations) have attracted a relatively scarce attention since such motions are infrared inactive, and therefore the only available evidence comes from NMR relaxation [2] or from collision induced far-infrared absorbtion or hyper-Raman measurements [3].

On the other hand, its high symmetry permits analysis of the molecular rotation in terms of a minimum set of parameters (one effective correlation time), so that it constitutes a natural benchmark where the available dynamical models can be tested.

Finally the predominantely coherent cross section for cold neutrons ($\sigma_{coh}/\sigma_{incoh} = 2.48$) makes it an interesting case in order to contrast the validity of most of the current approximations, as far as the specific effects of the liquid structure on the microscopic dynamics are concerned.

0953-8984/91/070851+13$03.50

2. Experimental details

The high-resolution quasi-elastic (QENS) experiments were carried out using the IRIS spectrometer of the ISIS pulsed neutron facility [4]. The achievable resolution using the (002) reflection of the analyser crystals was about 15 μeV over a Q-range from 0.25 to 1.85 Å^{-1}. For medium resolution measurements the (004) reflection of the spectrometer was used as well as the IN6 spectrometer located at the Institut Laue-Langevin [5].

The spectral data were converted into $S(Q,\omega)$ results by means of standard software and a slab correction was applied in order to take into account the attenuation due to chlorine absorbtion. The cells were mounted in variable-temperature, liquid helium cryostats (IN6) or a cooling bath (IRIS), and the temperatures were set to 260 K (15 K above the melting point) and 300 K.

The required thermodynamic and elastic constants have been calculated by making use of the parametrized equations given in the appendix of [6], and the diffusion coefficients used were set to the tracer diffusion values [7].

The static structure factors for the centre-of-mass distributions were computed from SSOZ approximations following the procedures described in [1], and the relevant molecular geometry parameters were set to values obtained from diffraction measurements [1].

3. Dynamical models

The total cross section can be written as a sum of elastic and inelastic contributions of both, coherent and incoherent proccesses

$$\left(\frac{\mathrm{d}^2\sigma}{\mathrm{d}\Omega\,\mathrm{d}\omega}\right)_{\mathrm{tot}} = \left(\frac{\mathrm{d}^2\sigma}{\mathrm{d}\Omega\,\mathrm{d}\omega}\right)^{\mathrm{el}}_{\mathrm{coh}} + \left(\frac{\mathrm{d}^2\sigma}{\mathrm{d}\Omega\,\mathrm{d}\omega}\right)^{\mathrm{el}}_{\mathrm{incoh}} + \left(\frac{\mathrm{d}^2\sigma}{\mathrm{d}\Omega\,\mathrm{d}\omega}\right)^{\mathrm{inel}}_{\mathrm{coh}} + \left(\frac{\mathrm{d}^2\sigma}{\mathrm{d}\Omega\,\mathrm{d}\omega}\right)^{\mathrm{inel}}_{\mathrm{incoh}} \tag{1}$$

The elastic contributions can then be expressed as a sum of coherent and incoherent parts as

$$\left(\frac{\mathrm{d}^2\sigma}{\mathrm{d}\Omega\,\mathrm{d}\omega}\right)^{\mathrm{el}}_{\mathrm{tot}} = N\frac{k_f}{k_i}\{u^2(Q)S_{\mathrm{coh}}(Q,\omega) + v^2(Q)S_{\mathrm{incoh}}(Q,\omega)\} \tag{2}$$

with

$$u(Q) = b^{\mathrm{C}}_{\mathrm{coh}} + 4\,b^{\mathrm{Cl}}_{\mathrm{coh}}\,b^{\mathrm{C}}_{\mathrm{coh}}\,j_0(Q\,r_{\mathrm{C-Cl}})$$

$$v(Q) = 2\,b^{\mathrm{Cl}}_{\mathrm{incoh}}\,j_0(Q\,r_{\mathrm{C-Cl}})$$

$$S_{\mathrm{coh}}(Q,\omega) = \frac{1}{2\pi}\int \mathrm{e}^{-\mathrm{i}\omega t}\,[I_d(Q,t) + I_s(Q,t)]\,\mathrm{d}t$$

$$S_{\mathrm{incoh}}(Q,\omega) = \frac{1}{2\pi}\int \mathrm{e}^{-\mathrm{i}\omega t}\,I_s(Q,t)\,\mathrm{d}t$$

where N represents the number of particles, k_f/k_i is the flux factor, $u(Q)$ and $v(Q)$ are molecular form factors referred to the molecular centre of mass, $I_d(Q,t)$ represents the intermediate scattering function encompassing all the coherent interference effects, and $I_s(Q,t)$ comprises the centre-of-mass motions.

Since the incident energies are too low to excite any of the sound modes (sound velocity about 5.94 meV at $T = 260$ K and incident energies of 3.12 meV) the coherent inelastic effects were assumed to be weak enough so that they should only contribute with a flat background. However, it was found necessary to include a narrow central lorentzian component with a linewidth given by the inverse of a relaxation time τ_m which measures the coupling between the translational motion and the internal molecular vibrational modes. The presence of such a mode is a well established fact in inelastic light scattering [6–8] and the values for those relaxation times were taken from table 1 of [6]. The linewidth which corresponds to such a mode is of the order of 1 μeV (i.e. τ_m is about 100 ps). It is then clear that no relevant information can be obtained from this component since the resolution required for such a purpose cannot be attained in the present set of experiments. Therefore, a contribution of the form

$$S_m(Q,\omega) = a_m \frac{\Gamma_m}{\omega^2 + \Gamma_m^2} \tag{3}$$

where Γ_m is the inverse of the τ_m relaxation times and a_m is the amplitude of this mode (taken from table 1 of [6]) which was added to the dynamical model.

The inelastic incoherent contribution was then modelled in a way analogous to the one employed in a previous work [9] so that the cross section may be written as

$$\left(\frac{\mathrm{d}^2\sigma}{\mathrm{d}\Omega\,\mathrm{d}\omega}\right)^{\mathrm{inel}}_{\mathrm{incoh}} = N\frac{k_f}{k_i}\exp\left(\frac{\hbar\omega}{2k_BT}\right)\sum_l (2l+1)\,v_l^2(Q)\int S'_{\mathrm{incoh}}(Q,\omega-\omega')\,S_l(\omega')\,\mathrm{d}\omega' \tag{4}$$

where the exponential is a detailled balance factor and $S_l(\omega)$ is a rotational relaxation function comprising all the details of the molecular reorientation.

The incoherent structure factor is related to the single particle function through

$$S'_{\mathrm{incoh}}(Q,\omega) = \exp\left(-\frac{\hbar\omega}{2k_BT}\right) S_{\mathrm{incoh}}(Q,\omega)$$

$$v_l^2(Q) = \sum_{v,v'=1}^{n} (b^v_{\mathrm{coh}}\, b^{v'}_{\mathrm{coh}} + (b^v_{\mathrm{incoh}})^2\delta_{vv'})\, j_l(Q\,r_v)\, j_l(Q\,r_{v'})\, P_l(\cos\theta_{vv'})$$

where the form factor $v_l(Q)$ is defined in terms of spherical Bessel functions with arguments given in terms of the distances to the centre of mass and the arguments of the Legendre polinomials are the angles between vectors connecting nuclei with the centre of mass.

The problem is now to specify models for centre-of-mass and rotational motions as well as to relate the coherent interference term with the incoherent single-particle function.

The first attempt to analyse the data was carried out with a previously used model [9] which had as the main ingredients a simple diffussion approximation for $I_s(Q,t)$, the Sköld approximation for $I_d(Q,t)$ and isotropic rotational diffusion for the inelastic incoherent part of the cross section. Several inconsistencies appeared when analysing the spectra using such a model.

First of all, rather poor fits were obtained when analysing the high-Q spectra, since the observed lineshape was found to deviate substantially from the model. On

the other hand, the rotational diffusion constants derived by means of such parametric fits to the measured spectra did show an anomalous temperature dependence since the values obtained for $T = 300$ K were consistently smaller than those for $T = 260$ K.

In order to overcome such difficulties several refinements had to be introduced. Two models were tested for the inelastic incoherent part. The first one is an adaptation of the itinerant oscillator model [10]

$$I_s(Q,t) = \exp(-Q^2\,\rho(t)\,t) \tag{5}$$

being

$$\rho(t) = \frac{k_B T}{M}\int_0^\infty f(\omega)\left(\frac{1-\cos\omega t}{\omega^2}\right)\mathrm{d}\omega$$

$$f(\omega) = \frac{2MD}{\pi k_B T}\exp\left(-\frac{\omega}{\omega_0}\right)^2 + A\omega^2\exp\left(-\frac{2\omega}{\omega_M}\right)$$

where the width function $\rho(t)$ is given in terms of the generalized frequency distribution $f(\omega)$ and the mean frequency ω_0 and ω_M have been computed from data given for methane by means of law of corresponding states [11].

As an alternative, the treatment due to Egelstaff and Schofield [12] provides a model with the correct asymptotic limits at low and high wavevectors in terms of a single parameter, the friction constant γ

$$I_s(Q,t) = \exp\left\{-DQ^2\left[\left(t^2+\frac{1}{\gamma^2}\right)^{1/2}-\frac{1}{\gamma}\right]\right\}. \tag{6}$$

Two models were tested regarding $I_d(Q,t)$. The first one, based on the well known approximation due to Sköld, breaks down at large Q values so that a more refined treatment was considered. The model due to Singwi in his study of coherent scattering from liquid argon [13], was found to be a valuable approximation for the distinct part of the intermediate scattering function. The resulting approximation is given as

$$I_d(Q,t) \simeq \sum_q \frac{Q^2\,k_B\,T}{2M}\frac{1}{\omega_q^2}\,L(R,Q)\,q^2\exp(-\mathrm{i}\omega_q t) \tag{7}$$

where

$$L(R,Q) \simeq \frac{R^3}{4\sqrt{Q\pi}}\int_0^\infty q'\,\mathrm{d}q'\,(S_{\mathrm{CM}}(q')-1)\exp\left(-\frac{R^2}{4}(Q-q')^2\right)\left(\frac{R^2}{2}(Q-q')^2-1\right).$$

The coherent interference effects are then collected into a function defined in terms of a correlation length R which is treated as a free parameter, and the structure factor for molecular centers.

In order to obtain realistic estimates of the rotational correlation times at the high temperature it was found necessary to include inertial effects, since it is well known from NMR results that the simple infinitesimal rotational diffusion model breaks down at $T = 300$ K. For such a purpose, we have used the rotational relaxation function [14]

$$S_l(t) = (\tau_- - \tau_+)^{-1}[\tau_-\exp(-t/\tau_-) - \tau_+\exp(-t/\tau_+)] \tag{8}$$

where

$$\tau_\pm = \tfrac{1}{2}(\tau_\omega^{-1} \pm 2\beta)$$

$$\beta = \tfrac{1}{2}(\tau_\omega^{-2} - 4\omega_j^2)^{1/2}$$

$$\omega_j^2 = l(l+1)\,k_B T/I$$

$$\tau_R = (\omega_j^2\,\tau_\omega)^{-1}.$$

Although two parameters enter into the above equation, one of them, corresponding to free inertial motion, is set to fixed value once the temperature and the moment of inertia I ($= 490 \times 10^{-40}$ g cm^2) are given.

3.1. Spectral components

The final formulae for the frequency dependence of the spectral components are as follows.

Translation.

$$S_0(Q,\omega) = \exp\left(-\frac{\langle\mu^2\rangle}{3}Q^2\right)\left\{\mu_{\text{coh}}^2 S_{CM}(Q)\,\frac{DQ^2}{\omega^2+(DQ^2)^2} + \frac{Q^2 k_B T}{12Mc^2}\,L(R,Q)f(\omega)\right.$$
$$\left. + v_{\text{incoh}}^2\,\frac{\exp(DQ^2/\gamma)}{\pi}\,\frac{DQ^2/\gamma}{[\omega^2+(DQ^2)^2]^{1/2}}K_1\left[\frac{[\omega^2+(DQ^2)^2]^{1/2}}{\gamma}\right]\right\} \qquad (9)$$

where the parameters to be fitted are then the amplitude entering the Debye–Waller factor, the coherence length and the friction constant γ. The symbol K_1 denotes a Bessel function of the second kind, and the values of the diffusion constant were set to those reproducing macroscopic and NMR data [15].

Rotation. The purely inelastic part thus becomes

$$S_r(Q,\omega) = \exp\left(-\frac{\langle\mu^2\rangle}{3}Q^2\right)\left[\sum_{l=1}^{\infty}(2l+1)\,v_l^2(Q)\,\frac{1}{\tau_- + \tau_+}\right.$$
$$\left.\times\left(\tau_-\frac{\Gamma_{\text{eff}}(Q)+\tau_-^{-1}}{\omega^2+(\Gamma_{\text{eff}}(Q)+\tau_-^{-1})^2} - \tau_+\frac{\Gamma_{\text{eff}}(Q)+\tau_+^{-1}}{\omega^2+(\Gamma_{\text{eff}}(Q)+\tau_+^{-1})^2}\right)\right] \qquad (10)$$

where $\Gamma_{\text{eff}}(Q)$ represents the value of the width function in the case of the itinerant oscillator model or the width of the incoherent translational part in the cases where the model due to Egelstaff *et al* was used. In the latter cases such a quantity was determined numerically and the rotational functions were assumed to be of Lorentzian shape in order to simplify the calculations.

The total structure factor is thus a sum of the translational part, a set of rotational Lorentzians and a contribution $S_m(Q,\omega)$ given by equation (3). The adjustable parameters needed to specify the model are then: the coherence length R and the friction constant γ for the translational part, and the relaxation time τ_ω characterizing the hindered rotation term (equation (10)), as well as a global scaling factor A_{sc}. The intensities to be compared with the experimental ones are then

$$I_{\text{model}}(Q,\omega) = A_{\text{sc}}[S_0(Q,\omega) + S_r(Q,\omega) + S_m(Q,\omega)] \otimes R(\omega) \qquad (11)$$

where the symbol $\otimes$ stands for the convolution operation and $R(\omega)$ is the resolution function measured with a vanadium standard.

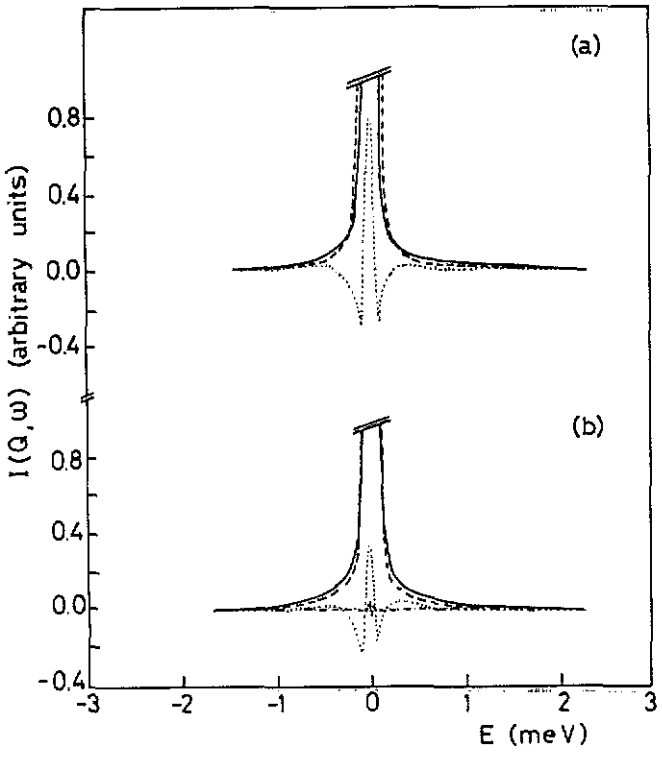

Figure 1. (*a*) Quasi-elastic neutron scattering from liquid CCl_4. The full curve represents the experimental spectrum at $Q = 0.53$ Å^{-1}; the broken curve the best fit using equation (2) (i.e. including only the $S_0(Q,\omega)$ purely translational part). The residuals for this fit are indicated by the dotted curve. (*b*) Symbols as in (*a*), but rotation was taken into account within a rotational diffusion aproximation (i.e. $S_0(Q,\omega) + S_r(Q,\omega)$). The chain curve represents the residuals from a fit using the rotational relaxation function given by equation (10), including also the narrow central Lorentzian (i.e. the full model given by equation (11)).

4. Results and discussion

The quasi-elastic spectra of liquid CCl_4 show rather unique characteristics compared with most of the spectra from other molecular systems and the most prominent features are discussed below.

In order to illustrate the necessity of developing the dynamical model briefly described in the previous section, figure 1 shows the best fits attainable using: (*a*) only translational components (cf equation (2)), and (*b*) a model including a rotational diffusion approximation. In the former case, it can be seen that a noticeable misfit is apparent in most of the spectral range, and although the fit improves in the latter one the intensity of the wings as well as the central intensity cannot be reproduced even if both, the friction and rotational diffusion constants are left unbounded. For the purpose of comparison, the residuals of a fit using the rotational model given by equation (10) are also shown in this figure. In this latter case the central narrow Lorentzian given by equation (3) is included with a relative weight given by the coefficients a_m which never exceeds 3.5% of the total integrated intensity. The overall agreement between the experimental and model intensities can be judged upon inspection of some

representative spectra shown in figure 2. All spectra for either IN6 or IRIS (002) and (004) reflections, and Q-values below 1.8 $Å^{-1}$ can be satisfactorily described in terms of the model discussed in the previous section. Above such a momentum transfer, small but systematic deviations appear, which show the apparent inability of such a basically hydrodynamic model to take into account subtle kinetic effects. Such deviations manifest themselves as misfits in the spectral wings in the energy transfer range of 0.2–0.4 meV.

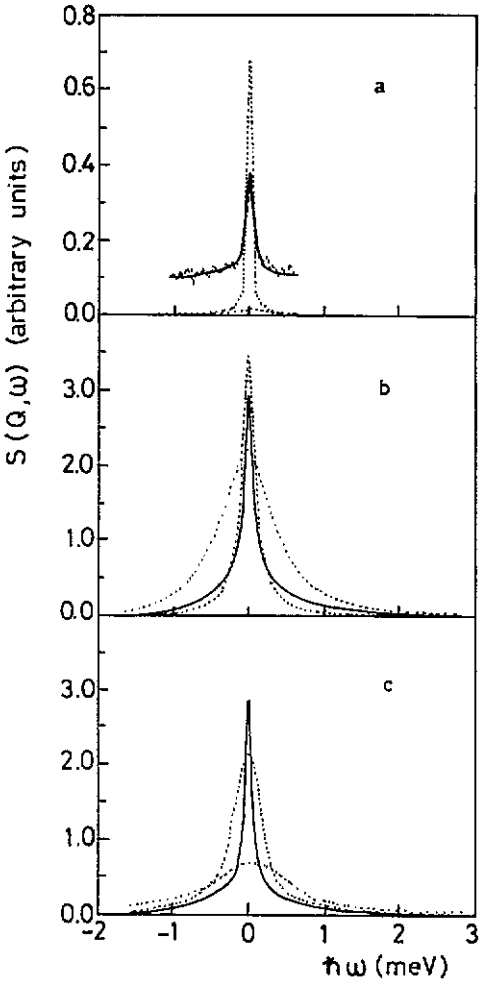

Figure 2. Representative spectra for an elastic momentum transfer value of Q = 0.53 $Å^{-1}$: (*a*) spectrum taken with the (002) analyser reflection of the IRIS spectrometer (T = 260 K); (*b*) spectrum from the IN6 spectrometer (T = 300 K); (*c*) also from IN6 (T = 260 K). The full curves represent the model fit and the experimental points are within the traces for spectra measured with IN6. The dotted curves show the total translational (narrow) and rotational (wide) contributions magnified five times.

4.1. Quasi-elastic widths

The Q-dependence of the quasi-elastic linewidths of both the coherent and incoherent contributions to the elastic cross section is shown in figure 3. As it can be seen, the incoherent contribution deviates from Fickian behaviour in both the itinerant oscillator and the Egelstaff–Schofield models. The main difference between the two models (apart from somewhat poorer fits in the case of the first model) lies in the distribution of spectral power. In the case of the oscillator model some intensity from

the elastic component is transferred to the inelastic wings; thus this model is unable to represent the central elastic intensity adequately. Therefore the subsequent results will refer to those obtained making use of the Egelstaff–Schofield model.

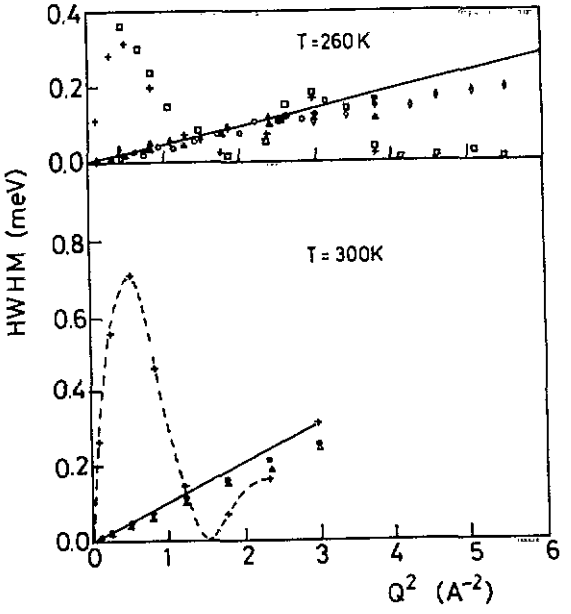

Figure 3. Half-widths of the translational components. Straight lines represent Fickian diffusion; Δ, IN6 data analysed with the itinerant oscillator model; ●, IN6 data analysed with the Egelstaff–Schofield formula; ◊, IRIS (004) data analysed with the Egelstaff–Schofield model; ○, as ◊ but IRIS (002); ×, half-widths of the coherent contribution (IN6); □, as × but from IRIS (004). In all cases a flat background representing less than 2% of the observed intensity at $\omega = 0$ was included in the fits.

The linewidths of the coherent contribution show a marked oscillatory behaviour with momentum transfer, as expected from the shape of the $L(R,Q)$ functions shown in figure 4. The surprising feature which makes such a behaviour resemble the well known results from liquified rare gases [16] is the persistence of noticeable oscillations over the whole momentum-transfer range investigated. The distance parameter R characterizing the extent of such oscillations (see equation (6)) could only be determined with a relatively large associated error, and the values derived from the different sets of measurements are given in table 1, as well as the fitted values for the friction constant γ. The large errors associated with the latter parameter when the results from different measurements are compared can be due to the small relative weigth of the incoherent structure factor with respect to its coherent counterpart.

The numerical values for the coherence parameter R entering the $L(R,Q)$ function can be compared with the extent of oscillations in the radial distribution functions given in a recent study on the temperature dependence of the structural properties of this liquid [17]. On the other hand, taking the values of about 5.3 Å for the distance between the centre-of-mass of neighbouring molecules, the values of the parameter R can be rationalized as a measure of strong dynamical correlations which involve about two shells of adjacent molecules at 260 K and only one at 300 K.

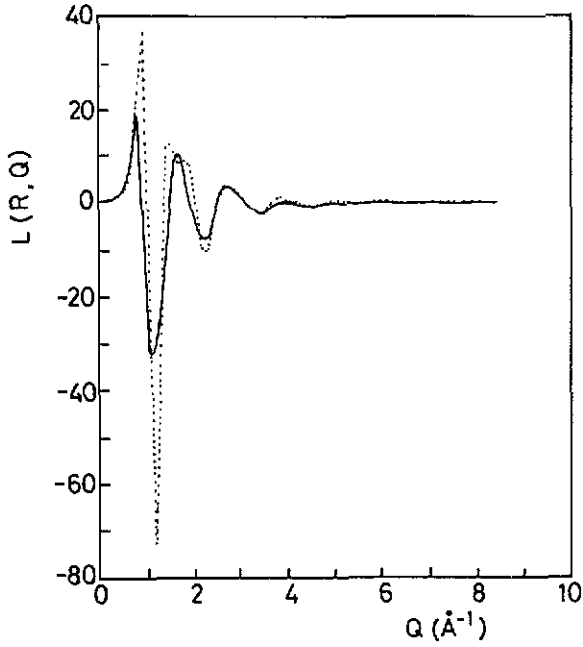

Figure 4. Values of the $L(R,Q)$ function for $T = 300$ K (full curve) and $T = 260$ K (dotted curve).

4.2. Rotational dynamics

The parameters characterizing the rotational motion are also given in table 1, as well as some representative results from NMR relaxation regarding the angular velocity and momentum correlation times. Before entering into the disscusion of the results found in this work it is worth commenting the reasons for the breakdown of the usual small-step isotropic rotational diffusion model in the case of this simple liquid.

From the analysis of the reported values for the correlation times for angular reorientation $\tau_{2,\theta}$ and angular momentum τ_J is possible to estimate the domain of validity of the simple diffusion approximation. First of all the deviations from the Hubbard relationship which must hold in the diffusion limit [18] can be gauged from the comparison of the last columns of table 1, where it can be seen that such limit conditions are nearly valid for $T = 260$ K but not at $T = 300$ K.

On the other hand, the value of τ_J in the strong-collision (diffusive) limit should approach the average collision interval (the magnitude listed in the last column of the table). Thus, it can be seen that such a condition does not hold even at low temperatures, although this last criterion of validity should be taken with care, due to the possible errors in the determination of the collision parameter Z.

The relevant dynamical parameters are then the correlation time τ_ω associated with angular velocities and intermolecular torques, and the free rotor time τ_{free} which is computed from the molecular moment of inertia and the temperature. The quantity to be compared with the NMR results is the correlation time τ_R corresponding to the second spherical harmonic, and as can be seen the obtained results are in good agreement with the previous NMR data. No rotational information was obtained from the data taken using the (002) reflection of the IRIS spectrometer,due to the restricted

Table 1. A summary of dynamical constants for CCl_4.

	Centre-of-mass motion			Rotational motion							
Instrument	γ [a]	R [b]	D_T [c]	τ_ω [d]	τ_{free} [d,e]	τ_R [c,f]	$\tau_{2,\theta}^{NMR}$ [c,g]	τ_J^{NMR} [c,h]	$I/6k_BT$	$\tau_\theta\tau_J$ [i]	τ_θ/Z [j]
IN6											
$T = 260$ K	1.59 (0.04)	17.1 (0.8)	0.30	0.0925 (0.02)	1.2	2.51	2.76 (0.15)	0.086 (0.008)	0.227	0.236	0.011
$T = 300$ K	1.44 (0.02)	10.6 (3.2)	1.49	0.103 (0.015)	1.1	1.91	1.72 (0.05)	0.133 (0.012)	0.197	0.229	0.009
IRIS (002)											
$T = 260$ K	1.80 (0.15)	16.2 (1.4)									
IRIS (004)											
$T = 260$ K	2.39 (0.81)	18.4 (2.6)		0.089 (0.041)	2.54						

[a] Units are 10^{12} s.
[b] Units are Å.
[c] Translational diffusion coefficient (in units of 10^5 cm^2 s^{-1}) from tracer diffusion [14]. The quantity in brackets corresponds to the computer simulation result given in [2].
[d] Units are 10^{-12} s rad^{-1}.
[e] Defined as $(I/k_BT)^{1/2}$.
[f] Corresponds to the $l = 2$ component in equation (7).
[g] Defined as the time required to rotate 1 rad, values taken from [2].
[h] Angular momentum correlation time, taken from [2].
[i] The Hubbard relationship [18] states that for the diffusion approximation to be valid requires $\tau_\theta\tau_J = I/6k_BT$.
[j] In the diffusion limit τ_J should correspond to the average collision interval $\tau_{2\theta}/Z$ where Z is the number of collisions per molecule and per second, taken from [6].

energy window of this configuration (the width of the rotational components is comparable to the spectral range). The rotational relaxation functions derived from this set of parameter values are depicted in figure 5.

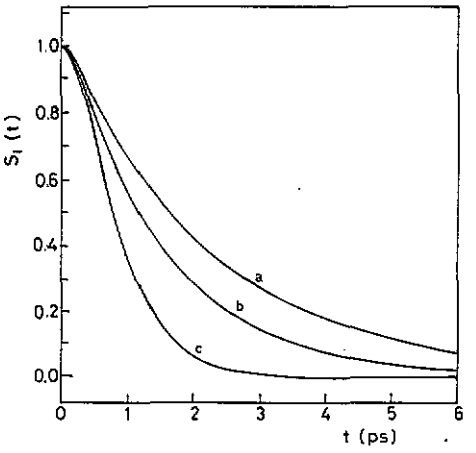

Figure 5. Rotational relaxation functions: curves a and b correspond to best-fit values for spectra measured with the IN6 instrument for $T = 260$ K and $T = 300$ K, respectively. Curve c corresponds to the estimation made using equation (10).

It is worth remarking that the rotational diffusion limit can be recovered if the conditions $\tau_R \gg \tau_\omega$ and $\omega_j^2 \tau_\omega^2$ hold, and that in this case one recovers a relaxation function with a single decaying exponential with a time constant τ_ω [14].

In order to test the sensitivity of the QENS spectra to small departures from sphericity predicted by some dynamical models [19] as well as that inferred from the analysis of far-infrared absorbtion bands, the following rotational function was also tested:

$$S_1(t) = \exp(-\gamma t)[\cos(\beta t) + (\gamma/\beta)\sin(\beta t)] \tag{12}$$

with

$$\gamma = \tfrac{1}{2}\tau_\omega^{-1}$$
$$\beta = \tfrac{1}{2}(4\omega_j^2 - \tau_\omega^{-2})^{1/2}$$

and with ω_j^2 retaining the same meaning as in equation (7).

Such a function represents a slow modulation regime [14] and therefore was used to explore the possibility of detecting subtle oscillatory features in the angular velocity autocorrelations at $T = 260$ K. Rather similar values for τ_ω were found when analysing a set of spectra (about 0.24 ps rad^{-1}) and the fit was noticeably worse with this approximation. Furthermore, the value of the τ_ω rotational constant shows a tendency towards the limit of validity of the slow modulation regime, i.e $4\omega_j^2 > \tau_\omega^2$, thus indicating the adequacy of the fast modulation formula to represent the reorientational dynamics of this liquid. For the purpose of comparison the corresponding relaxation function is also shown in figure 5.

5. Conclusions

The QENS spectra of liquid carbon tetrachloride, a mostly coherent scatterer, has been analysed by making use of a relatively simple dynamical model where the only addi-

tional information required apart from static structure data is a coherence parameter which was left free in the fitting procedure. The numerical values for such a quantity are in agreement with what is known about the extent of orientational correlations from diffraction data.

The present paper thus extends some recent efforts to derive sound physical information from the inelastic scattering of predominantely coherent samples [20].

It has been shown that the QENS spectra are sufficiently sensitive to detect the departures from the idealized small-step rotational diffusion, and that such departures can be taken into account by means of an extended model which becomes analogous to the rotational diffusion model in a fast-modulation limit. The use of such a model should be preferred to the simple diffusion model, since only one adjustable parameter is needed in both cases.

Although considered in a number of papers on theoretical and computer simulation, no departures from sphericity in the rotational reorientation of this liquid could be detected. Since the spectra have been shown to be quite sensitive to fine details of the molecular dynamics, such effects, if present, have to be of a rather small magnitude, which makes them extremely difficult to detect with the present spectroscopic techniques.

In summary, it can be asserted that the approximations followed in this paper can be used profitably for the analysis of the rotational motion withouth having to make use of the Kerr approximation as has been recently postulated [21].

A further set of experiments using very high-resolution techniques (i.e. neutron spin-echo) is envisaged in order to analyse in greater detail the very-low-frequency components (the central narrow Lorentzian) and the results will be reported in due time.

Acknowledgments

This work was supported in part by DGICYT grant No PB89-0037-C03. Excellent assistance in the preparation of the manuscript was given by Mr A Gomez. The technical staff of the ISIS facility gave us invaluable help during the experimental runs and with data analysis.

References

[1] Bermejo F J, Enciso E, Alonso J, Garcia N and Howells W S 1988 *Mol. Phys.* **64** 1169
See also Steinhauser O and Neumann M 1980 *Mol. Phys.* **40** 115

[2] Lindman B and Forsen S 1976 *NMR: Basic Principles and Progress* vol 12, ed P Diehl *et al* (Berlin: Springer) ch 2
Gillen K T, Noggle J H and Leipert T K 1972 *Chem. Phys. Lett.* **17** 505

[3] See, for instance, Shin S and Ishigame M 1988 *J. Chem. Phys.* **89** 1892 for recent hyper-Raman results and Joslin C G and Gray C G 1989 *Chem. Phys. Lett.* **154** 369 for a recent treatment on collision induced spectra.

[4] *ISIS User Guide, Experimental Facilities at ISIS* 1988 *Rutherford-Appleton Laboratory Report* RAL-88-030

[5] Blank H and Maier B (eds) 1988 *Guide to Neutron Research Facilities at the ILL* Grenoble, France

[6] Samios D and Dorfmuller Th 1980 *Mol. Phys.* 41 637

[7] Taken from figure 4 of Hildebrand J H 1978 *Faraday Discuss. Chem. Soc.* **66** 151

[8] Mountain R D 1968 *J. Res. NBS* A **72** 95

[9] Bermejo F J, Batallan F, Enciso E, White R, Dianoux A J and Howells W S 1990 *J. Phys.: Condens. Matter* **2** 1301
[10] Sears V F 1965 *Proc. Phys. Soc.* **86** 953
[11] Sears V F 1966 *Can. J. Phys.* **44** 867
[12] Egelstaff P A 1967 *An Introduction to the Liquid State* (New York: Academic) p 129
[13] Singwi K S 1965 *Physica* **31** 1257
[14] Rothschild W G 1984 *Dynamics of Molecular Liquids* (New York: Wiley) p 172
[15] See Collings A F and Mills R 1970 *Trans. Faraday Soc.* **66** 2761 for numerical data on self-diffusion constants in addition to those from [7].
[16] Sköld K, Rowe J M, Ostrowski G E and Randolph P D 1972 *Phys. Rev.* A **6** 1107
Egelstaff P A, Gläser W, Litchisnki W, Schneider E and Suck J B 1983 *Phys. Rev.* A **27** 1106
[17] Misawa M 1989 *J. Chem. Phys.* **91** 5648
[18] Hubbard P S 1963 *Phys. Rev.* **131** 1155
[19] Lynden-Bell R M 1984 *Molecular Liquids: Dynamics and Interactions (NATO ASI Series C 135)* ed W J Orville-Thomas *et al* (Dordrecht: Reidel) p 501; for details of a recent computer simulation carried out with a model system exhibiting such oscillations see Rau A and Gerling R W 1990 *Z. Phys.* B **78** 275. Results obtained from the analysis of far-infrared absorbtion giving this type of oscillatory behaviour can be found in Davies G J and Evans M 1976 *J. Chem. Soc. Faraday Trans.* II **72** 1194.
[20] Dahlborg U, Gudowski W and Davidovic M 1989 *J. Phys.: Condens. Matter* **1** 6173
[21] Wei D and Patey G N 1989 *J. Chem. Phys.* **91** 7113